

Developing a ground based mass balance approach  
for estimating CH<sub>4</sub> emissions from  
anthropogenic sources  
Abdulkarim Mohammed

SC/CHEM 4000 8.0 Research Project

Fall/Winter 2016/2017

Developing a ground based mass balance approach  
for estimating CH<sub>4</sub> emissions from  
anthropogenic sources

Abdulkarim Mohammed

Research Supervisor: Dr. Robert McLaren

Course director: Derek Wilson

York University

4700 Keele Street Toronto

Ontario M3J 1P3

**Abstract.**

Methane (CH<sub>4</sub>) emissions from anthropogenic sources are not well quantified. A mass balance technique is used to estimate surface methane emissions at the Keele Valley Landfill site in Vaughan, Ontario. A Picarro Cavity Ringdown Spectroscopy (CRDS) instrument is used in this project. Three mobile studies are conducted on November 29, 2016, February 22, 2017, and March 09, 2017 to measure the horizontal flux estimate. The average CH<sub>4</sub> emissions estimate is  $6.0(\pm 1.6) \times 10^3$  kg/hr. This average emissions estimate is significantly higher than the previously reported emissions inventory of this facility, which estimates that the landfill emits  $2.4 \times 10^3$  kg/hr. The CRDS instrument is also intercompared with another analyzer, the Unisearch Tunable Diode Laser Spectrometer (TDL), to determine the feasibility of using both instruments in future mass balance emissions estimates.

## Table of contents

Abstract.....	3
Table of contents.....	4
1. Introduction.....	5
2. Experimental.....	10
2.1 Picarro G-2401 CRDS .....	11
2.2 Unisearch RP-101 TDL.....	13
2.3 Mobile study.....	13
2.4 Mass balance method.....	16
3. Results and Discussion.....	17
3.1 Intercomparison study.....	17
3.2 Mobile study of landfill site.....	25
3.2.1 November mobile study.....	25
3.2.2 February mobile study.....	29
3.2.3 March mobile study.....	32
4. Conclusion and future work.....	36
5. References .....	37

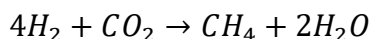
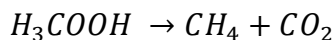
## **1. Introduction**

Methane is an important anthropogenic greenhouse gas which is responsible for around 20% of global warming since preindustrial times. Its global warming potential over a 100-year period is 28, compared to 1 for CO<sub>2</sub> (IPCC., 2012). That means that methane traps 28 times more heat than CO<sub>2</sub> per mass unit. Since the pre-industrial era, methane concentrations have increased by 150% (Hausman et al.,2016)., mainly driven by an increase in anthropogenic activities such as the extraction and burning of fossil fuel along with other sources discussed below. For a decade since 1997, global methane mixing ratios witnessed a period of near zero growth. Since then however, methane mixing ratios have risen steadily at a rate of 4 ppb/yr. and emissions growing at a rate of 6 Tg/yr., according to the latest assessment report by the intergovernmental panel on climate change. The reasons behind these two trends are not well understood, partly due to a lack of accurate monitoring (Verhlost et al., 2016). With better monitoring practices, the recent trends of methane concentrations can be better understood. Methane can also play an important role in climate change mitigation efforts, especially given the fact that its lifetime is 9.6 years, much shorter than that of CO<sub>2</sub> of 55.6 years (Hausmann et al., 2016)

The troposphere is the lowest portion of the earth's surface, containing 85% of the atmosphere's mass. It extends anywhere from 6 to 20 km from the earth's surface, depending on the latitude. The lowest part of the troposphere is the planetary boundary layer (PBL), which is directly influenced by its contact with the planetary surface. The PBL changes in height from tens of meters to almost 2km, depending on several factors such as time of the day, location, solar heating, etc. The PBL plays an important role in controlling the concentration of trace gases emitted from the surface, and will directly impact our measurement of methane flux at the landfill site

Per the IPCC assessment report, the global methane budget from 2000 to 2009 included 553 Tg/yr. in sources and 550 Tg/yr. in sinks, which was a top-down estimate [IPCC,2014]. A bottom up estimate from the same time period had 678 Tg/yr. in sources and 632 Tg/yr. in sinks[IPCC.,2014]. Typically, top-down estimates depend on measured patterns of variability in atmospheric observations, whereas bottom-up methods require estimated emissions by combining activity data with emissions factors.

Roughly 40 percent of methane sources are attributed to natural sources. Wetlands account for the vast majority of natural methane production. Wetlands are areas with high water saturation and low soil fertility (Bubier et al.,1994). Another characteristic of wetlands is low oxygen concentration, which creates an ideal environment for fermentation. Two important fermentation reactions that account for natural methane production are as follows;



Other natural sources of methane include termites, permafrost melting and wildfires. Termites break down biotic components, primarily producing ethanol with methane as a by-product. Permafrost is geological land located in high altitudes (e.g. the arctic) that has been frozen for a period of several years to several thousand years. With global warming leading to rising temperatures, permafrost regions are melting at an increased rate, releasing more of the methane that has been trapped inside (Schuur et al., 2015). Combined, these three sources account for 43 Tg/Yr., or 19 % of natural methane sources. [IPCC.,2014]

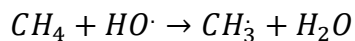
Anthropogenic sources of methane account for 60% of the methane emissions into the atmosphere (Sreeniyas et al., 2016). In general, there are 3 major processes of methane production. By far the largest source of anthropogenic methane is agriculture and waste. Agriculture has witnessed the largest growth of emissions, particularly with regards to rice cultivation and industrial farming (Ruddiman, 2003). Worldwide rice cultivation has grown rapidly due to the continuously rising global population. Rice paddies are characterized by water-logged soil and warm weather, which act like wetlands. However, these wetlands are anthropogenic as they serve the global food production. Another source of agricultural methane is ruminants from farm animals. Ruminant animals such as cows and sheep contain bacteria in their GI-tract which helps break down the food they digest and thus, methane is produced as a by-product. But since farm animals also serve the global food production, they are considered an anthropogenic source of methane. Landfill waste is another important methane source, accounting for roughly 10% of man-made methane emissions. Landfill waste undergoes anaerobic decomposition by methanogens (Themelis et al., 2007).

The second type of anthropogenic methane is pyrogenic methane which is mainly associated with extracting and burning of fossil fuels, which account 28% of anthropogenic methane emissions. Although oil accounts for some methane emissions, much of pyrogenic methane is attributed to the production and processing of natural gas. Methane emissions also occur in other sectors of the natural gas industry such as storage, transmission, and distribution. Methane leaks throughout the distribution networks of natural gas are a significant source of methane emissions, and are a target of climate mitigation strategies (Phillips et al., 2012).

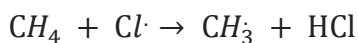
The third type of anthropogenic emissions is pyrogenic methane in the form of biomass burning. Biomass burning is the incomplete burning of both living and dead organic matter such as

vegetation. Most instances of biomass burning are human induced, including the burning of vegetation for the purpose of land-clearing. Biomass burning accounts for roughly 9% of anthropogenic methane emissions.

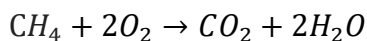
Part of the global methane budget includes methane sinks. The most important methane sink, accounting for almost 95% of all sinks, is tropospheric hydroxyl radical (OH·) and chlorine Cl· radicals (IPCC, 2001). The major removal mechanism of methane from the atmosphere involves the following reaction with a hydroxyl radical;



The products of this reaction are methyl radicals, which eventually produce formaldehyde, and water. As well as being the primary sink of methane, this reaction serves as one of the most important sources of water vapour in the upper atmosphere. Moreover, this reaction gives methane its average lifetime of 9.6 years. Chlorine radicals also serve as a methane sink. The removal mechanism of chlorine radicals is known as a free radical halogenation. The first step is given in the following reaction;



Like the reaction with the hydroxyl radical, the final stable organic product of this reaction is formaldehyde. Apart from hydroxide and chlorine radicals, soils represent a minor sink for methane. Methanotrophic bacteria are a group of bacteria that reside in soils and use methane as a source of carbon during oxidation. The methane oxidation reaction of methanotrophic bacteria in soils are as follows;



The instrumental methods used to measure methane in this study are Cavity ring-down spectroscopy (CRDS) and Tunable Diode Laser Spectroscopy (TDLS). Both instrumental techniques use laser absorption spectroscopy, which uses lasers to determine the concentration of gas species using absorption spectroscopy. Absorption spectroscopy is an analytical technique which uses the unique absorption spectroscopy of a gas in the UV-Visible or infrared portions of the electromagnetic spectrum. When methane interacts with laser light, the sample absorbs energy from the radiating field. The intensity of the absorption depends on the frequency of the laser, and is used to quantify the concentration of the trace gas. The detailed schematic of both instruments will be discussed in the experimental.

The CRDS instrument can be used to estimate the total emissions of a species released from a point source. One method of estimating the emissions is known as the mass balance technique. This technique relies on the principle that the CH<sub>4</sub> mole fraction down wind of the emissions source is greater than the mole fraction up wind from it (Karion et al., 2013). If the increase in mole fractions is integrated across the width of the emissions plume within the planetary boundary layer, measured by an aircraft for example, we can measure the surface emissions of methane, provided the horizontal wind speed and wind direction are steady. This method has recently been used to quantify the methane emissions from large oil and gas regions in USA and Canada (Gordon et al., 2015, Baray et al., 2017). One of the uncertainties of this approach is the limitation of the aircraft to get close enough to the surface to characterize the surface concentrations of CH<sub>4</sub>. Therefore, we are developing a mobile mass balance approach which involves driving nearby the emissions source in order to get a more accurate surface estimate. However, this approach has the opposite limitation of the aircraft method, as it cannot measure

CH<sub>4</sub> mixing ratios at high altitude, where the trace gas is presumed to be well mixed. This might produce an estimate which is significantly higher than the true value.

The purpose of this study is to measure an emissions estimate of CH<sub>4</sub> from the Keele Valley Landfill site using a version of the aircraft mass balance technique. A Picarro G-2401 Cavity Ring-Down Spectroscopy (CRDS) will be used to measure CH<sub>4</sub> enhancements downwind of the source with background measurements upwind of the source as well. The wind data and boundary layer height for this emissions estimate approach will be acquired from nearby weather stations and airports. The CRDS instrument was also be used along with a Unisearch RP-101 TDL instrument to quantify methane concentration at the York University Keele campus. The data from both instruments were intercompared and analyzed for their correlation in order to determine the viability of using the TDL instrument in future mass balance emission estimates.

## **2. Experimental**

As part of our study, data was collected over a period of 5 months (September- November 2016, February-March 2017). During that time, local air was sampled from the CAC Air Quality Research Station on the roof of the Petrie Science and Engineering building at York University. In order to measure the mixing ratio of CH<sub>4</sub>, two instruments were used, a Cavity Ringdown spectroscopy instrument (Picarro G2401), and a Tunable Diode Laser Analyzer (Unisearch-RP101)). The Picarro was able to measure CO, CO<sub>2</sub> and CH<sub>4</sub> and H<sub>2</sub>O simultaneously while the TDLS could only detect one gas at a time, either CH<sub>4</sub> or CO<sub>2</sub> depending on the laser installed. Both instruments gathered data continuously with sampling times of 2 seconds (Picarro) and 0.1 s to 10 s (Unisearch RP101). This section will focus on their principle of operations

## 2.1 Picarro G-2401 CRDS

The Picarro Cavity Ring-down spectrometer relies on the fact that almost all gas phase molecules have a unique vibrational absorption spectrum in the near-infrared region, which appears as a series of sharp, well defined lines with a known wavelength value. This allows the concentration of any species to be determined by measuring the height of the absorption peak. The Picarro G-2401 consists of a continuous wave (CW) tunable diode laser, a cavity defined by 3 highly reflective mirrors (Figure 1), and a photodetector. The larger set-up also includes a vacuum pump which serves as an outlet gas flow, as well as data collection and analysis electronics (e.g. a monitor). The laser emits a beam which enters the cavity. The laser light quickly circulates around the cavity as it bounces from one mirror to the next. The mirrors do not reflect at 100%, creating a phenomenon whereby the laser beam slightly leaks and the signal intensity of the laser decreases with time. The photodetector placed outside the cavity detects the leak and produces a signal that is directly proportional to the signal intensity of the laser in the cavity. Once the photodetector signal reaches a threshold, the laser stops emitting CW and the light entering the cavity is shut down. Without any input, the wave that's present in the cavity experiences a rate of decay known as the ring-down time that depends on losses within the cavity (loss on mirrors, scattering, and absorption). When a gas species is introduced to the cavity, absorption decreases the ring-down time. It is the ringdown time that is the analytical signal in CRDS as opposed to a traditional absorption signal. The following graph demonstrates the difference in ring-down time when an absorbing species is introduced within the cavity.

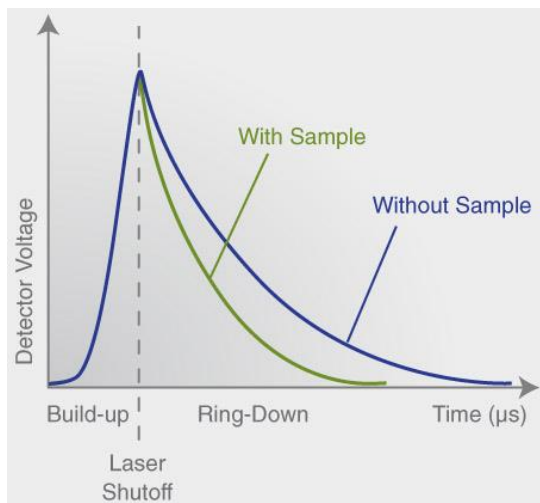


Figure 1.1: Light intensity as a function of time with and without the presence of a sample, (Picarro, [http://www.picarro.com/technology/cavity\\_ring\\_down\\_spectroscopy](http://www.picarro.com/technology/cavity_ring_down_spectroscopy))

The CRDS then measures the difference between the ring-down time with the gas species and the ring-down time without any gas species. This allows quantitative and precise measurements of the concentration of the gas species.

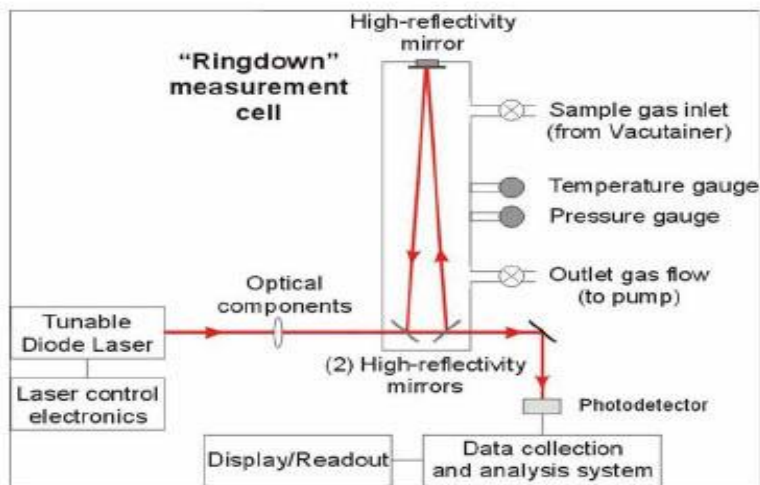


Figure 1.2: Schematic of a Cavity Ring-down spectrometer using a three-mirror optical cavity. (Wahl et al.,2006)

## 2.2 Unisearch RP-101 TDL

The other instrument used for the intercomparison was the Unisearch RP-101 tunable diode laser. It is in somewhat similar to the Picarro CRDS, in that they both use near IR ( $\sim 1.6 \mu\text{m}$ ) absorption spectroscopy. The TDL setup consists of a tunable laser source, transmitting optics, long path absorbing medium (i.e. air sample), a retroreflector, collection optics as well as a detector. The laser source emits a wave that is tuned to match an absorption line of the species of interest ( $\text{CH}_4$ ). When the species is present in the path of the laser, the signal intensity of the emitted wave decreases. A detector (photodiode) then measures the difference in signal intensity and determine the concentration of the species using the beer lambert law, which is as follows;

$$A = \log_{10} \frac{I_0}{I} = \epsilon lc$$

## 2.3 Mobile Study

To complement the regular sampling of air from the Keele campus, a total of 3 road studies were conducted on separate days (November 29<sup>th</sup> 2016, February 22<sup>nd</sup> 2017 and March 9<sup>th</sup> 2017). The purpose of those studies was to measure methane mixing ratios and the methane horizontal flux along the Keele valley landfill. The Picarro (CRDS) was used for this study. The study involved packing the CRDS, as well as the vacuum pump onto a vehicle. A YETI 1250 portable power station with auxiliary marine battery was used to serve as the power supply, with a capacity equivalent to 6 hours of study time. The Picarro CRDS instrument (with computer), GPS, and

monitor consumed about 240 W power. The CRDS was connected to an PFA inlet sample line (1/4 "OD, ~ 3 m length) mounted outside and on the forward passenger side of the vehicle (2015 Toyota Prius) to sample the air, and an LCD monitor to observe the data in real time (see picture below)A mobile meteorological station was used at a location ~ 2 km north of the landfill site, and a handheld GPS device was used to record the precise location of the vehicle at all times, a requirement when calculating the methane flux.



Image 1: Set-up of the mobile study

The study involved driving several north-south and east-west transects downwind of the landfill site. The following figure shows the location of the study, as well as the direction of the different transects

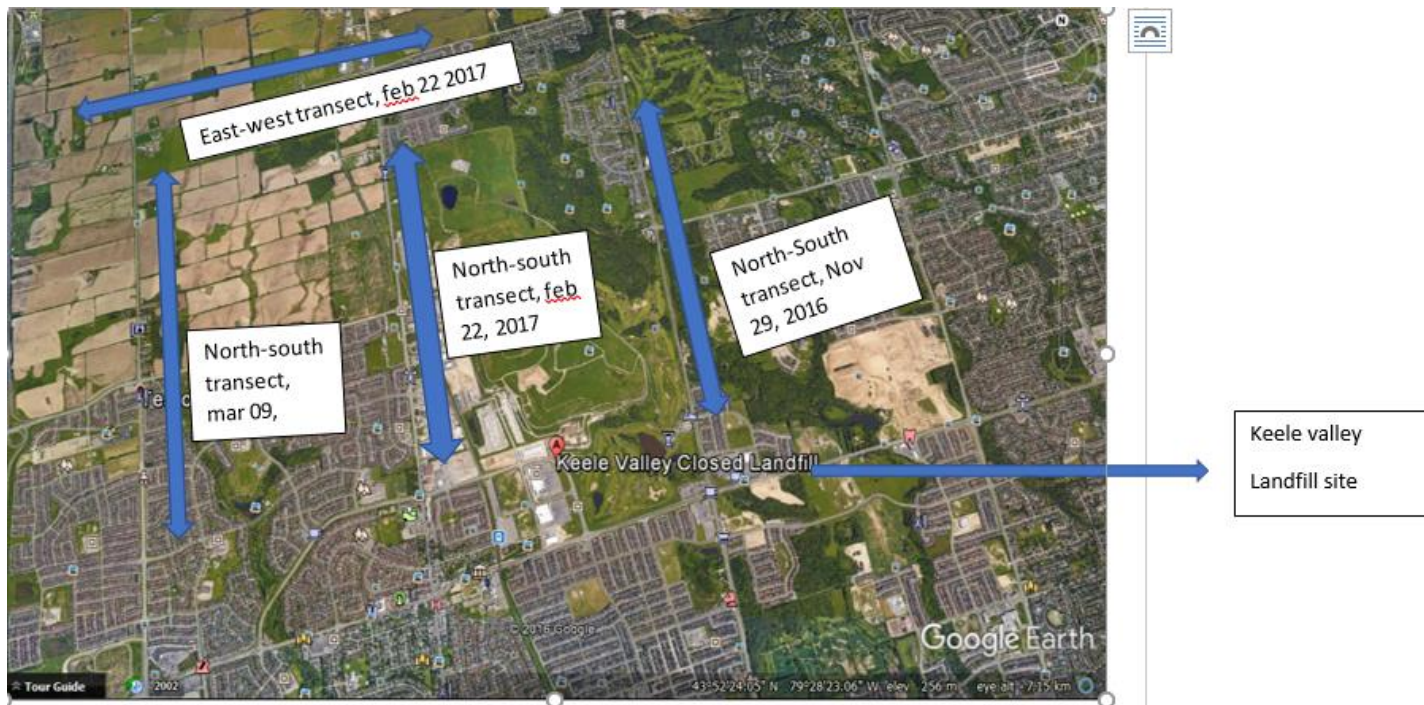


Figure 2.1, Map of the Keele Valley Landfill and the surrounding area

The initial period of the study (November 29, 2016) involved driving around the landfill site to look for enhancements in the CH<sub>4</sub> mixing ratio. These elevated readings were witnessed in certain sections of the drive-around which were downwind of the landfill, which could be explained by the wind direction for that day. Subsequently (Feb 22 & Mar 09, 2017), a series of transects were driven once the area of elevated emissions was located. The north-south transect along Dufferin Street adjacent to the landfill was approximately 4km long, stretching southbound from the intersection of Keele & Kirby to Keele & Major McKenzie. The east-west transect spanned approximately 3km east of Jane St. & Kirby St. Using the elevated mixing ratios

recorded by the CRDS analyzer, a methane horizontal flux was calculated using the mass balance technique.

## 2.4 Mass Balance Method

A mass balance technique has been used to quantify the total emissions of trace gases, including methane, released from large area sources (Peischl, J, et al., 2016; Gordon et al., 2015, Baray et al, 2017)). This technique has been used extensively to measure methane enhancements in emission sources such as oil and gas fields using aircraft. This method has three assumptions; steady horizontal winds, a well-developed planetary boundary layer, and measurements sufficiently downfield from the emissions source. The flux calculation involves calculating the mole fraction of the methane by subtracting the background mixing ratio from the enhancement, and integrating it across the horizontal plume in the planetary boundary layer (i.e. the transect length). The flux calculation is derived from;

$$flux = v \cdot \cos(\alpha) \int_{z_0}^{z_1} \int_{-y}^y (X - X_{bg}) dy \cdot dz$$

Where  $v$  is the magnitude of the wind velocity normal to the direction of the road over the course of the transect,  $Z_1-Z_0$  is the planetary boundary layer, the  $(X - X_{bg})$  being the methane enhancement above the background, and the  $y/-y$  value is the distance along the transect. The background  $CH_4$  is usually defined as the mixing ratio immediately outside the source of emission. The  $(\alpha)$  component is the angle between the mean wind direction and the direction normal to the transect (aircraft or vehicle path), so that  $\cos\theta \cdot dx$  is the increment perpendicular to the mean horizontal wind direction. The product of the mass balance integration is calculated in kilograms per hour, knowing the molecular weight of  $CH_4$ .

### **3. Results and discussion**

#### **3.1 Intercomparison study**

An intercomparison study was conducted on October the 8<sup>th</sup>, 9<sup>th</sup> and 10<sup>th</sup>. During those three days, the TDL instrument was adjusted to take CH<sub>4</sub> instruments, whereas the Picarro was simultaneously measuring 4 trace gases including CH<sub>4</sub>. The TDL was programmed to take measurements at 0.1 second dwell time, compared to a 2 second measurement for the Picarro CRDS. A time series of methane mixing ratios from both instruments is shown in Figure 3.1. Since they had different measurement times, the data was averaged into 1 minute intervals throughout the whole 24-hour cycle, which meant averaging 600 data points for the TDL (0.1 sec) and 30 data points for the CRDS (2 sec). That was done using the pivot table function on Microsoft excel. Another adjustment made prior to plotting the graphs was matching the time zones for both instruments. The TDL was measuring data at local time, whereas the CRDS measured and stored data in UTC. Before we could compare both data sets, we adjusted the CRDS to local time by subtracting the time of every data point by 4 hours. A correlation graph between the two data sets averaged to 1 minute intervals is shown in Figure 3.2.

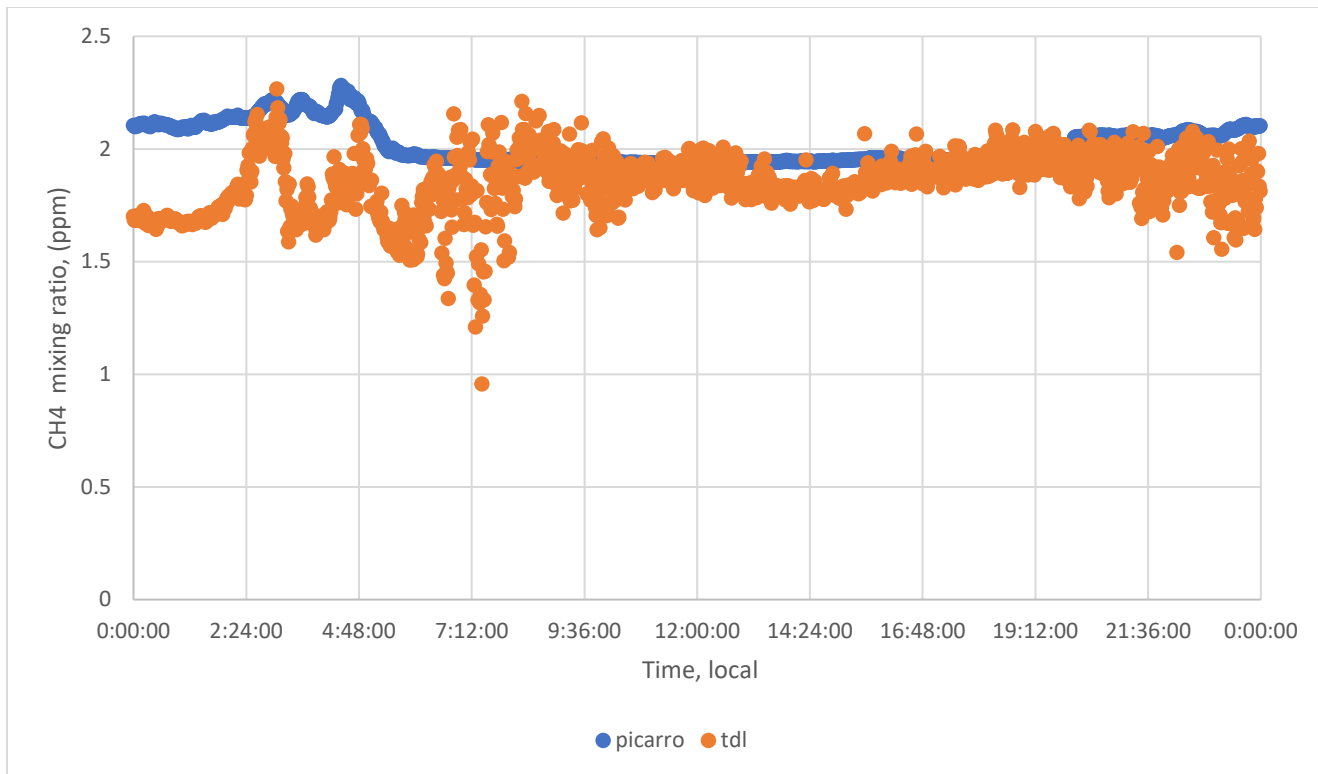


Figure 3.1: Time series graph of CH<sub>4</sub> mixing ratio by the TDL and Picarro CRDS on 08.10.2016

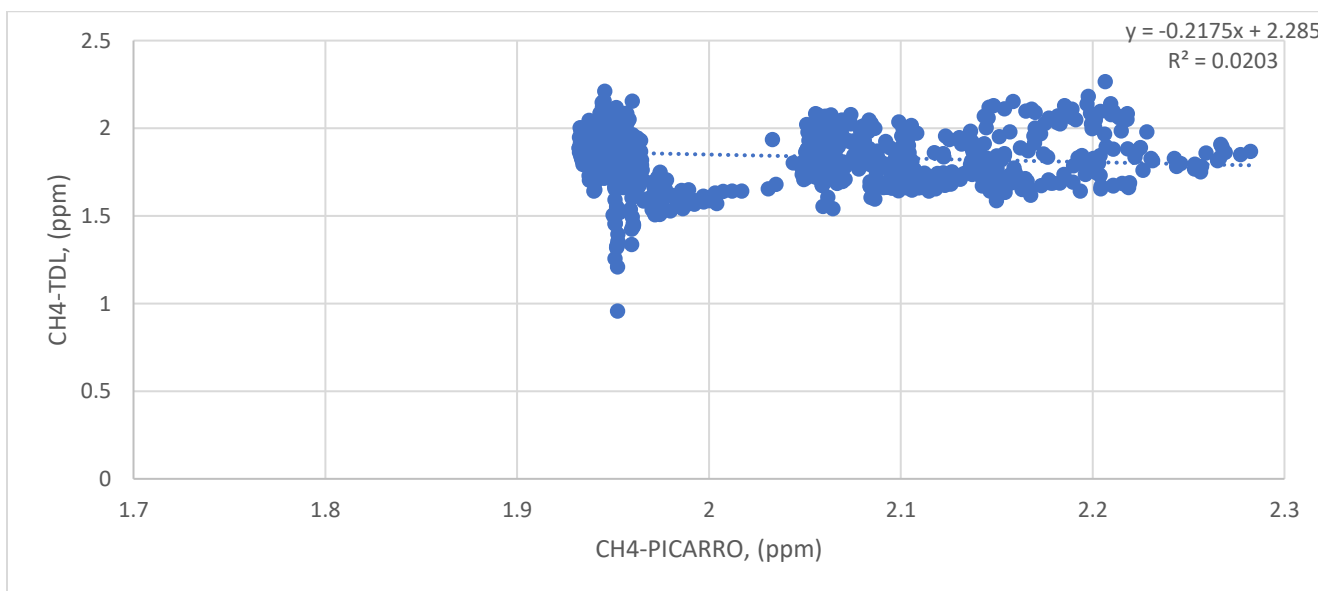


Figure 3.2: Correlation graph between the TDL and Picarro CRDS on 08.10.2016

Table 3.1: average concentration, number of data points, and other statistical metrics for the intercomparison on 08.10.16

08.10.16	PICARRO CRDS	TDL
	CH4 (Dry)	CH4
Average, ppm	2.01	1.84
Data points	1440	1440
St.dev, ppm (1-2pm)*	0.00199	0.0347
Median, ppm	1.95	1.83
Minimum, ppm	1.93	0.93
Maximum, ppm	2.29	2.29

\*A measure of instrumental precision was made by calculating the standard deviation during a period where methane was not changing concentration (1-2pm)

One of the striking features of the CRDS data set is the low noise and the high degree of stability. Qualitatively, one can notice how stable the CRDS CH<sub>4</sub> data was throughout the whole 24-hour cycle. On this particular day there was little diurnal profile for the CH<sub>4</sub> mixing ratio. The standard deviation of the two instruments is compared in certain times of the day when CH<sub>4</sub> mixing ratios is relatively constant. Quantitatively, the standard deviation values for 1 hour periods of time in the middle of the day were 0.00199, 0.00218, and 0.00210 ppm for the CRDS . In contrast, the standard deviation values for the TDL instrument in the same periods were 0.0375, 0.0143 and 0.0139 ppm respectively, which is larger than the CRDS values by a factor of 10, on average.. By minimizing the atmospheric variability, the largest source of the standard deviation is the instrumental variability. The TDL appears to have a higher noise throughout the intercomparison.

The intercomparison graph plotted on October the 8<sup>th</sup> shows very little correlation between the 2 instruments. There is an increase in methane mixing ratios which traces back to the previous night (our plot begins at 00:00). Both the TDL and the CRDS record that rise, which continues until around 05:00. The most likely cause for that rise in mixing ratio is surface emissions into a shallow nocturnal boundary layer, compared to a much higher mixed layer during the day. In the evening, the boundary layer decreases significantly, leading to a less efficient mixing of gases in the atmosphere. The result of that is an increase in the mixing ratios of methane. Conversely, there is a drop in the mixing ratios at around 5 am, which is when the nocturnal boundary layer starts to rise gradually. By sunrise the boundary layer is much higher and the methane concentration drops accordingly. This is reflected by the measurements by both instruments, with mixing ratios hovering below 2 ppm for the rest of the day. At around 19:00 ppm, we witness a similar rise in methane mixing ratios. This coincided with the sunset (16:50 pm) on that particular day, which means that the rise in methane ppm was attributed to the decrease in the nocturnal boundary layer.

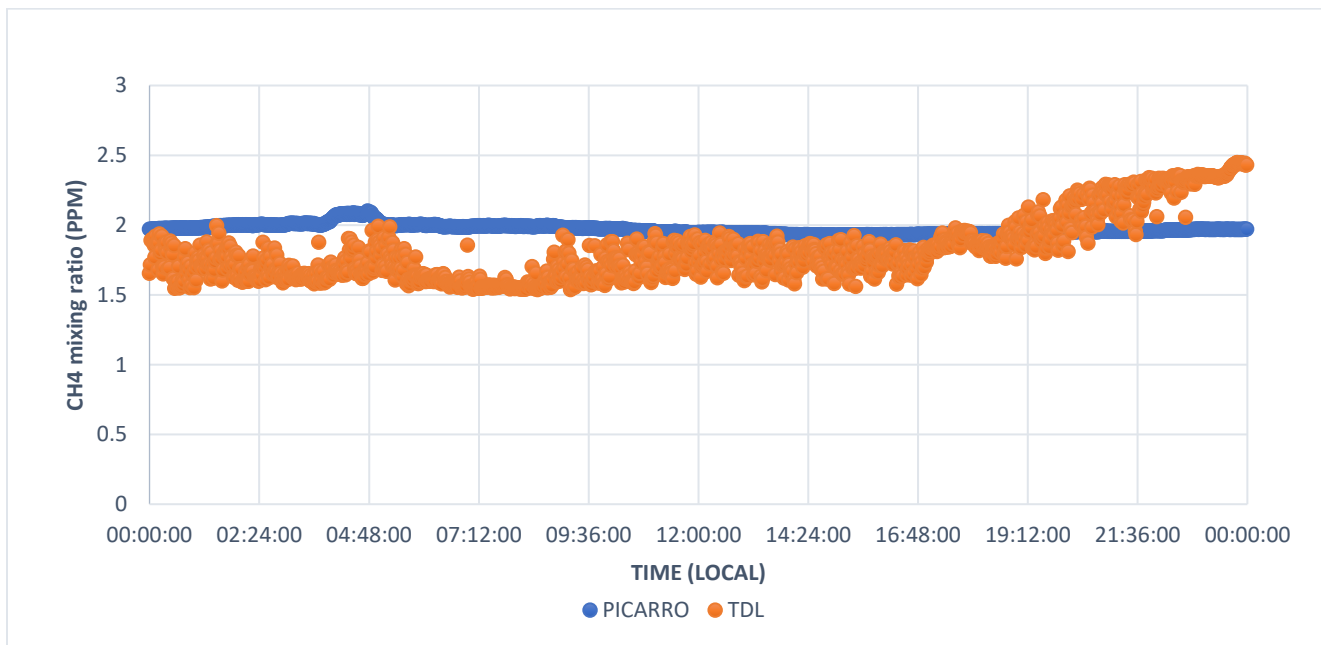


Figure 3.3: Time series graph between the TDL and the Picarro CRDS on 09.10.2016

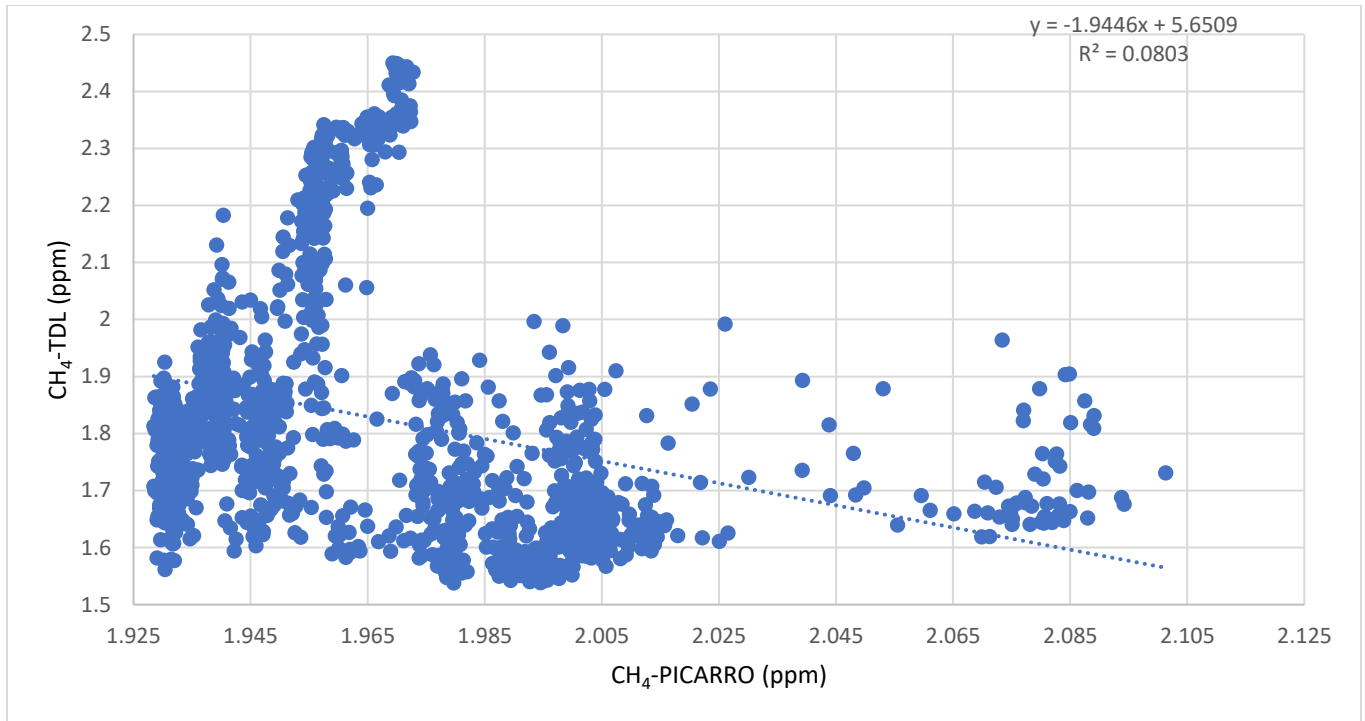


Figure 3.4: Correlation graph between the TDL and the Picarro CRDS on 09.10.2016

Table 3.2: Average concentration, number of data points, and other statistical metrics for the CRDS and TDL on 09.10.16

09.10.16	PICARRO CRDS	TDL
	CH4 (dry)	CH4
Average, ppm	1.97	1.82
Data points	1440	1440
St.dev, ppm (7pm-8pm) *	0.00218	0.0143
Median, ppm	1.96	1.70
Minimum, ppm	1.92	1.27
Maximum, ppm	2.10	2.97

\*A measure of instrumental precision was made by calculating the standard deviation during a period where methane was not changing concentration ( 7-8pm)

The data on the 9<sup>th</sup> of October did not display the same atmospheric variability in methane mixing ratios. According to Figure 3.3, the CRDS graph had a narrow fluctuation, with a difference in 0.15 ppm between the highest and lowest values. The TDL graph has a more visible diurnal trend, with the methane values rising after 19:00 to almost 2.5 ppm.

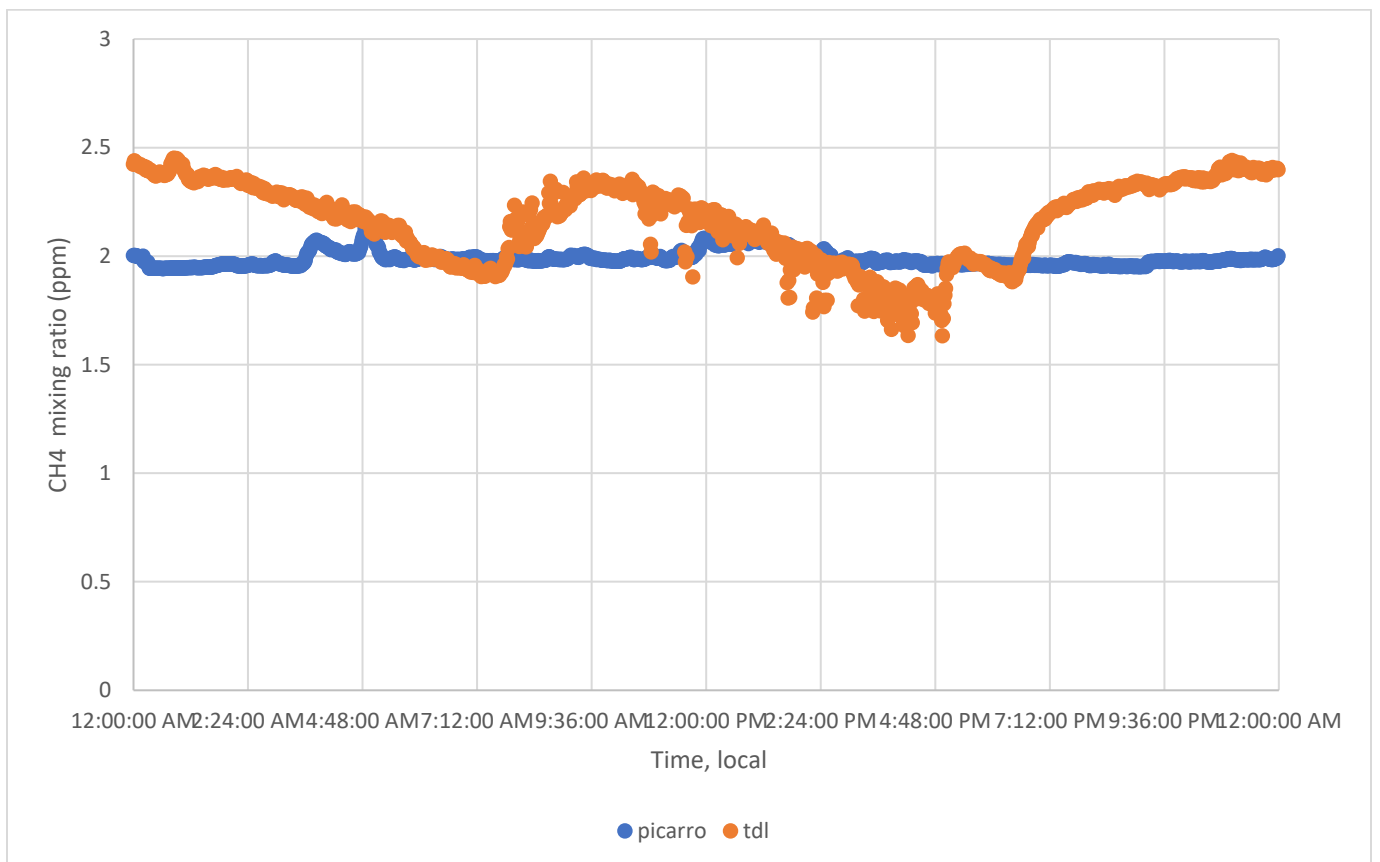


Figure 3.5: Time series graph between the TDL and the Picarro CRDS on 10.10.2016

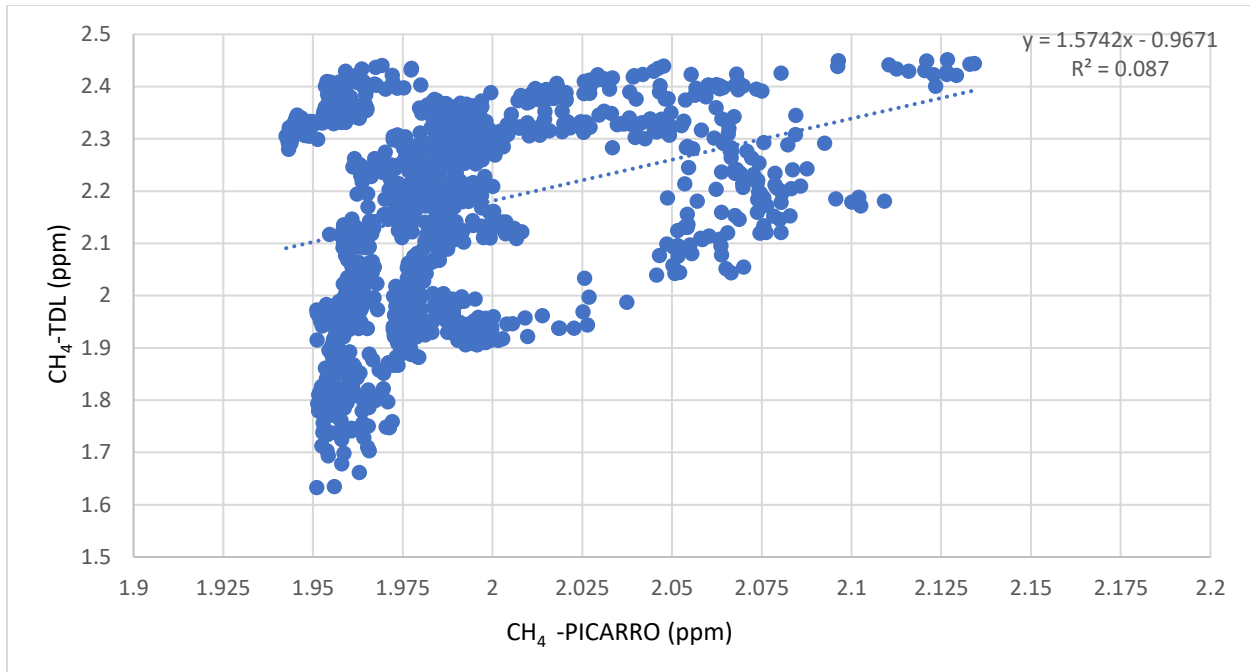


Figure 3.6: Correlation graph between the TDL and the Picarro CRDS on 10.10.2016

Table 3.3; Average concentration, number of data points, and other statistical metrics intercomparison on 10.10.16

10.10.16	PICARRO CRDS	TDL
	CH4 (dry)	CH4
Average, ppm	1.98	2.16
Data points	1440	1440
St.dev, ppm	0.00210	0.0139
Median, ppm	1.98	2.20
Minimum, ppm	1.94	1.63
Maximum, ppm	2.13	2.45

\*A measure of instrumental precision was made by calculating the standard deviation during a period where methane was not changing concentration (10-11pm)

We see a similar trend on October the 10<sup>th</sup>, where the Picarro only fluctuates by 0.19 ppm throughout the diurnal cycle. The TDL fluctuates by 1.66 ppm, although much of that is attributed to the drift in the instrument itself.

One important observation of the intercomparison graphs is the lack of correlation between the two instruments. The R-squared values for the three days were 8.2%, 8.1% and 7.87%. These values indicate minimal correlations. There are several reasons for this phenomenon, including the low reflectivity of the retroreflector used in the experiment. Our retroreflector had aluminum coating, which has a lower reflectivity in the region of methane absorption than gold. Based on the coating curve from the manufacturer, the aluminum coated analyzer has a reflectivity of 85% in the 1.6  $\mu\text{m}$  wavelength. In comparison, the absorption curve of a gold-coated retroreflector is around 95% at the 1.65  $\mu\text{m}$  wavelength region (citation). A gold retroreflector was purchased later in the term and has much better performance (not included in this project) than the aluminum retroreflector measurements indicated here. Another source of error in this dataset could be night-time condensation of water on the retroreflector, resulting in loss of precision and accuracy. In contrast, the CRDS is a point source measurement with a 3-meter inlet tubing used to detect the CH<sub>4</sub> concentration at a point. Based on the poor correlation values of the two instruments, and the significant noise in the TDL, it would not be feasible to use an aluminum coated retroreflector in future mass balance estimate emissions.

### 3.2 Mobile study of landfill site

A road study was conducted on three separate days to identify the landfill as a major source of methane and to calculate an emission estimate of methane from the Keele Valley landfill site.

The first study was conducted on the 29<sup>th</sup> of November 2016, followed by two mobile studies in February and March to estimate CH<sub>4</sub> emissions estimate from the landfill site.

#### 3.2.1 November Mobile Study

A preliminary mobile study was conducted on November 29, 2016 to investigate methane emissions at the Keele Valley landfill site in Vaughan, Ontario. The study involved driving along the landfill site and measuring enhancements in CH<sub>4</sub> mixing ratios. The location of the mobile study is shown in Figure 3.6



Figure 3.6: Map of the Keele Valley Landfill Site

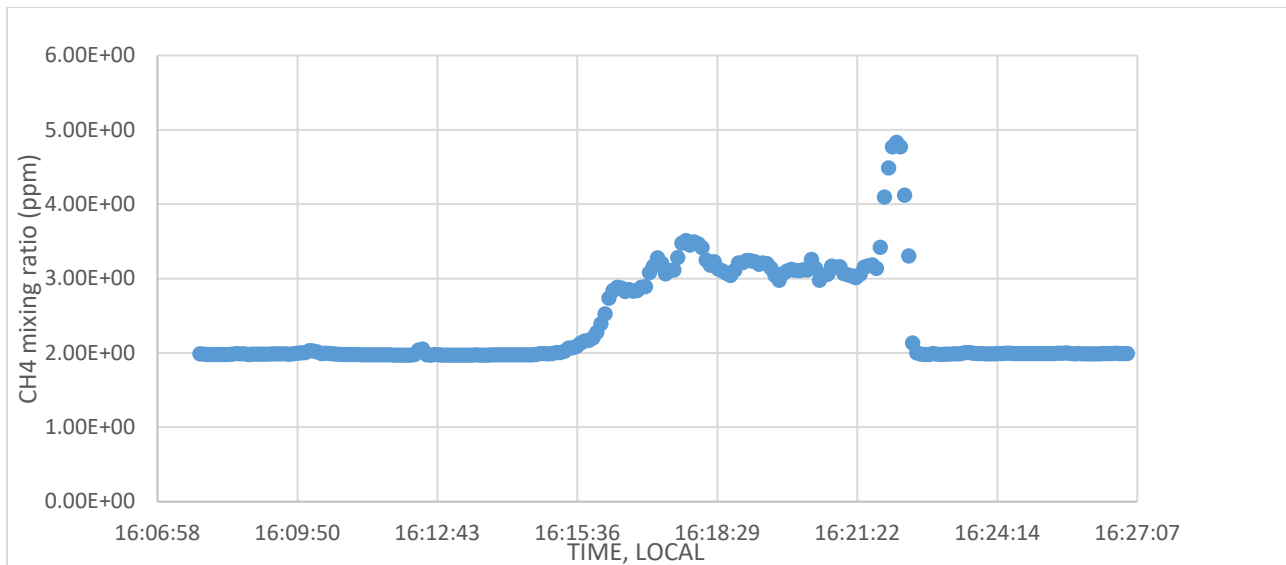


Figure 3.7: Time series plot of methane enhancement for landfill study on 29.11.16 while driving south on Dufferin Street

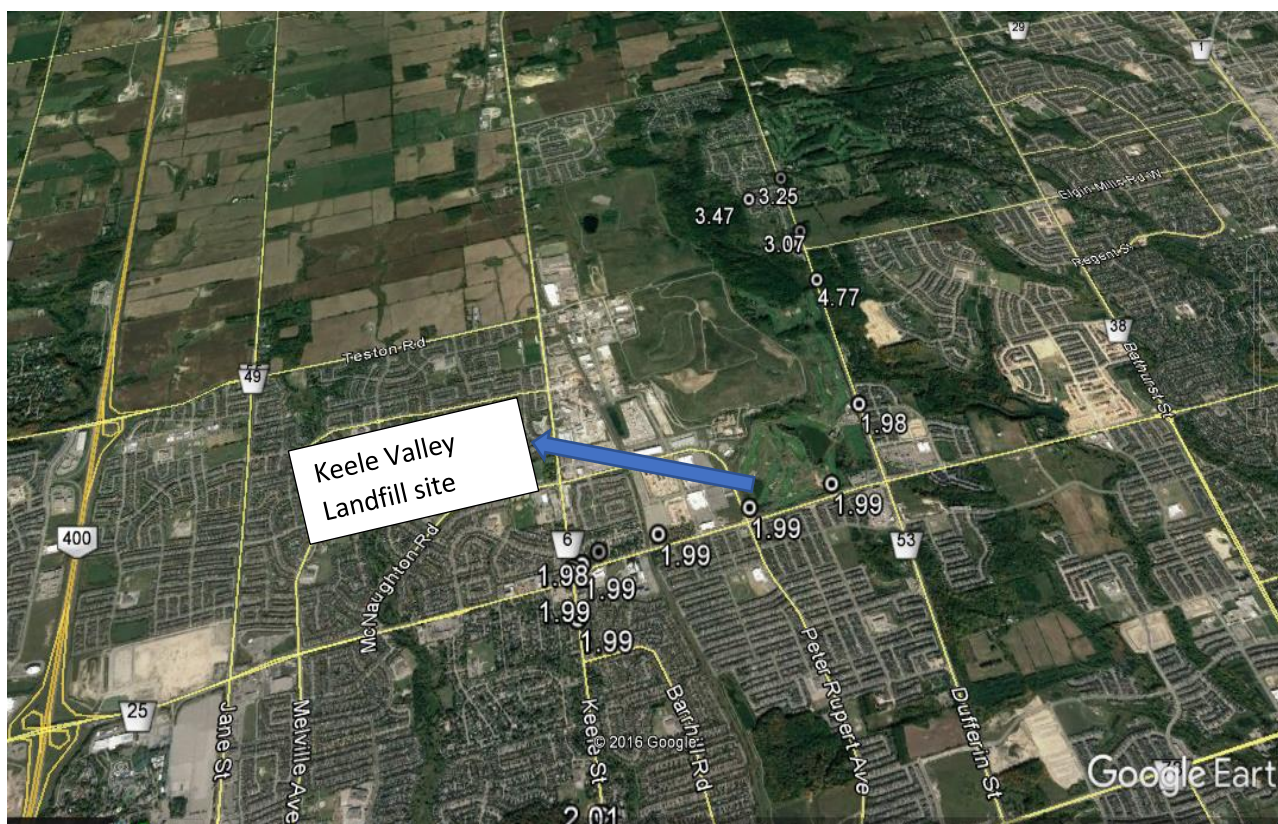


Figure 3.8: CH4 mixing ratio both inside and outside the enhancement region (ppm)

Table 3.4: flux information for landfill study on 29.11.16;

Transect #	Wind direction, ( $^{\circ}$ ) ( $\pm 10^{\circ}$ )	Wind speed, m/s	Transect length, km	Planetary boundary layer, m ( $\pm 50$ m)	Cosine theta value	CH4 flux, ( $\times 10^3$ Kg/hr)
1	220	3.5	4.126	50	0.765	14.8

We could confirm the presence of a significant methane source at the landfill, as evidenced by the large enhancement in CH4 mixing ratios, well above background compared to the measurement taken from the drive to the landfill and back from York University. A basic flux estimate calculation was also made using the data from the site, along with wind data from a nearby meteorological station. Equation 1, the mass balance equation is as follows;

$$flux = v \cdot \cos(\alpha) \int_{z_0}^{z_1} \int_{-y}^y (X - X_{bg}) dy \cdot dz$$

Where ( $v$ ) represented the wind speed and ( $\alpha$ ) represented the angle between the wind direction and the direction normal to the road. Both the wind speed and the wind direction were acquired from the King City Weather station nearby. Therefore,  $\cos(\alpha)$  was acquired by using the cosine function as well as the angle between the wind vector and the normal to the road. The first integral ( $\int_{z_0}^{z_1} dz$ ) corresponded to the Boundary layer component of the equation, which was determined using a constant homogeneous boundary layer height. For this preliminary estimation, which is highly uncertain, because the nocturnal boundary layer was starting to develop during the drive, we estimated the surface effective boundary layer to be 50m. For subsequent days we used Aircraft Meteorological Data and Relay (AMDAR) data, to determine

Boundary Layer heights by using the temperature profile of commercial aircraft landing and taking off at nearby airports. The second integral ( $\int_{-y}^y (X - X_{bg}) dy$ ) represented the CH<sub>4</sub> enhancement relative to the background mixing ratio over the width of the plume, multiplied by the mole fraction of CH<sub>4</sub> and the number density of air. The background value is determined by averaging the mixing ratios along the road that is upwind of the emissions source, as shown in Figure 3.6. The width of the plume was determined using the GPS coordinates from our hand-held device, whose time was synchronized with that of the CRDS by adjusting for the response time of the instrument (12 seconds). Therefore, every CH<sub>4</sub> measurement had a corresponding GPS coordinate, which was used to calculate the width of the plume by converting the longitude and latitude values to distance in meters. Using these components, the mass balance equation was used to get a horizontal flux estimate.

The emissions estimate on that study was  $14.8 \times 10^3$  kg/hr, which is a highly uncertain value, largely due to the uncertainty in the effective boundary layer height. The CH<sub>4</sub> plume was characterized by a very large enhancement in CH<sub>4</sub> mixing ratio (see Fig 3.7), which we wanted to identify the source of. The highest CH<sub>4</sub> concentration was recorded at 16:22 pm (4.83 ppm). Using the time on the GPS and adjusting for the response time of the CRDS. (12 seconds), the GPS coordinates of that particular data point was located and mapped onto Google Earth. The mapping showed that the measurement was taken at an area of the road that had an angle of approximately  $210^\circ$  from the stack at the power plant which is located at the southern end of the landfill site. That was within the uncertainty range of our wind direction ( $220 \pm 10^\circ$ ). The power plant is used to burn CH<sub>4</sub> from the landfill to convert it into electrical power. Therefore, the large enhancement in CH<sub>4</sub> could be traced back to incomplete combustion of CH<sub>4</sub> in the gas

turbines, as well as possible CH<sub>4</sub> leaks in the pipelines feeding the generation plant at that location.

There were other sources of uncertainty in the emissions estimate. One of the assumptions in the mass balance technique is the presence of a well mixed planetary boundary layer. The methane enhancements on that study were recorded from approximately 16:15 pm to 16:25 pm, with sunset being at 16:43 pm. The nocturnal boundary layer begins to form at that time of the day, which created a rise in the urban background methane. This was evident by the increase in the background level of methane of around 200 ppb (1.9ppm to 2.1 ppm) as we returned to York University compared to our transit to the site earlier in the afternoon. Therefore, it is difficult to assume that there was a well developed planetary boundary layer or nocturnal boundary layer during this particular mobile study. Another assumption to make when calculating the flux estimate is the measurements being taken sufficiently downfield from the emission source. The road study on that day was focused on identifying the source of methane, which involved driving right along the landfill site. The maximum distance between the CRDS instrument and the landfill was 1.1 km, which is not sufficiently downfield from the methane source. Therefore, having confirmed the presence of a significant source of methane, and the viability of calculating a horizontal flux estimate, further studies were conducted in that area, designed to mitigate the sources of error which contributed to the uncertainties in the first emissions estimate.

### **3.2.2 February Mobile Study**

A second mobile study was conducted on February 22<sup>nd</sup> to get a more accurate emissions estimate. Along with the CRDS and the GPS device, we also used a mobile meteorological station to get more localized weather data. The CH<sub>4</sub> enhancement region was downwind of the

landfill (see Figure 3.9), whereas the background mixing ratio was determined by measuring the CH<sub>4</sub> values upwind of the landfill site. The location of the downwind transects (both north south and east west) and the upwind background transect (east west) with respect to the landfill site is shown in Figure 3.9.

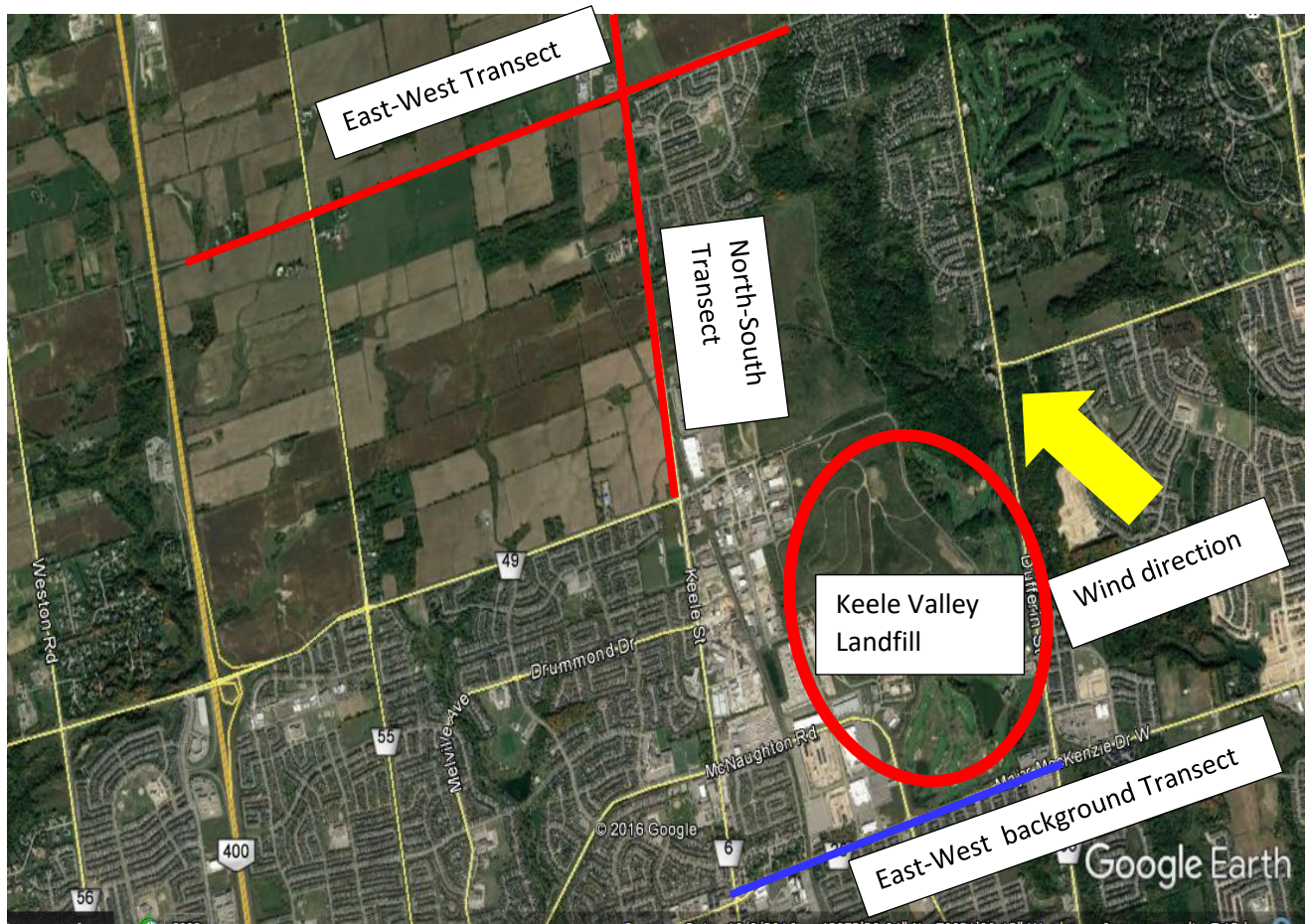


Figure 3.9: Map of the landfill site in the mobile study (Feb 22,2017)

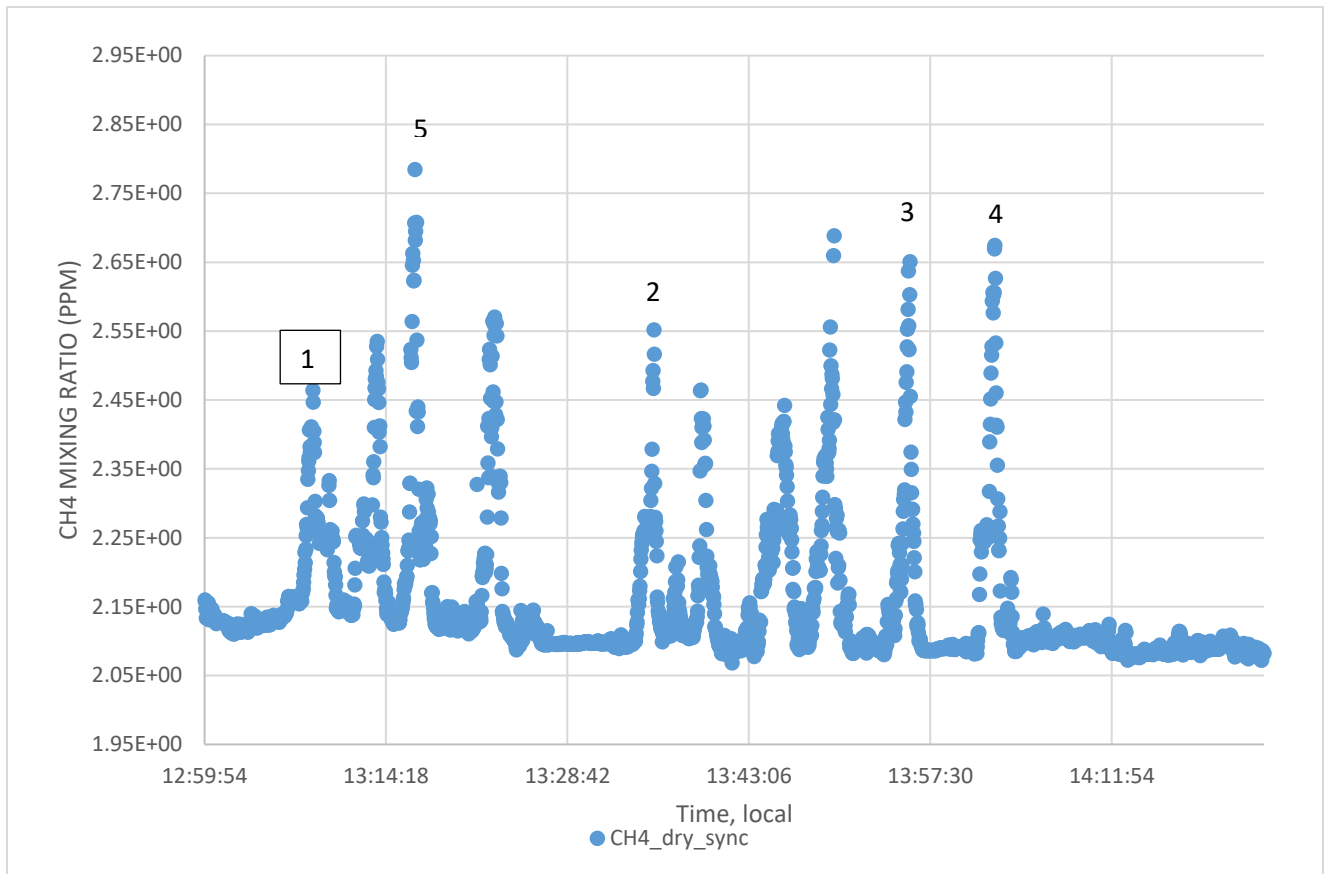


Figure 3.10: Time series plot of CH<sub>4</sub> mixing ratios along the Keele Valley Landfill Site, Feb 22, 2017 (transects labeled)

Table 3.5: Emissions estimate for landfill study on 22.02.17

Transect #	Wind direction, (°) (±10)	Wind speed, m/s (±0.1 m/s)	Transect length, km	Planetary boundary layer, m (±150m)	Cosine theta value	CH <sub>4</sub> flux, (×10 <sup>3</sup> Kg/hr)
1 (East-West)	125	2.8	3.25	300	0.798	7.2
2 (North-South)	125	2.8	2.66	300	0.798	3.9
3 (North-South)	125	2.8	2.01	300	0.707	5.8
4 (North-South)	125	2.8	3.96	300	0.707	5.7
5 (East-West)	125	2.8	3.1	300	0.707	6.2

The background mixing ratios was determined by driving upwind of the landfill site, whereas the CH<sub>4</sub> enhancements were recorded when driving downwind relative to the landfill. The weather on that mobile study was hazy and cloudy, resulting in a lower boundary layer height. The meteorological data used in equation 1 was retrieved from our own meteorological (met) station as well as the King City Weather Station. The boundary layer height was estimated using AMDAR data, whereas the CH<sub>4</sub> enhancement was measured using the CRDS data along with the GPS coordinates of each data point, adjusted for CRDS response time. Using equation 1 of the mass balance technique, the emissions estimate of 5 transects (see peaks 1 to 5 in Figure 3.10) in this mobile study is shown in Table 3.8. The average CH<sub>4</sub> emission estimate was  $5.8 (\pm 2.6) \times 10^3$  kg/hr, with the minimum estimate of  $3.9 \times 10^3$  kg/hr and a maximum of  $7.2 \times 10^3$  kg/hr. These estimate values are significantly lower than the values calculated on the first mobile study in November, but expected to be more accurate. Although the data from this mobile study is more accurate, there is still a high degree of uncertainty. The largest source of uncertainty is the wind direction. Our met station was placed at an uneven surface at the site of the study, with close proximity to passing cars. This resulted in highly uncertain values of wind direction. Therefore, the ( $\alpha$ ) component of equation 1 was calculated using a combination of the met station data as well as the weather station at King City. A third mobile study was conducted in March in order to get an emissions estimate when the weather was relatively clearer.

### **3.2.3 March mobile study**

A similar mobile study was conducted on March 9<sup>th</sup>, 2017 where we measured CH<sub>4</sub> enhancements in the downwind region and calculated an emissions estimate. This time, the location of our transect routes were different to that of the study in February, owing to the different wind directions. In order to minimize the error involved with using two conflicting

weather stations, we relied solely on the weather station at King City. Figure 3.11 shows the transect route with respect to the landfill site.

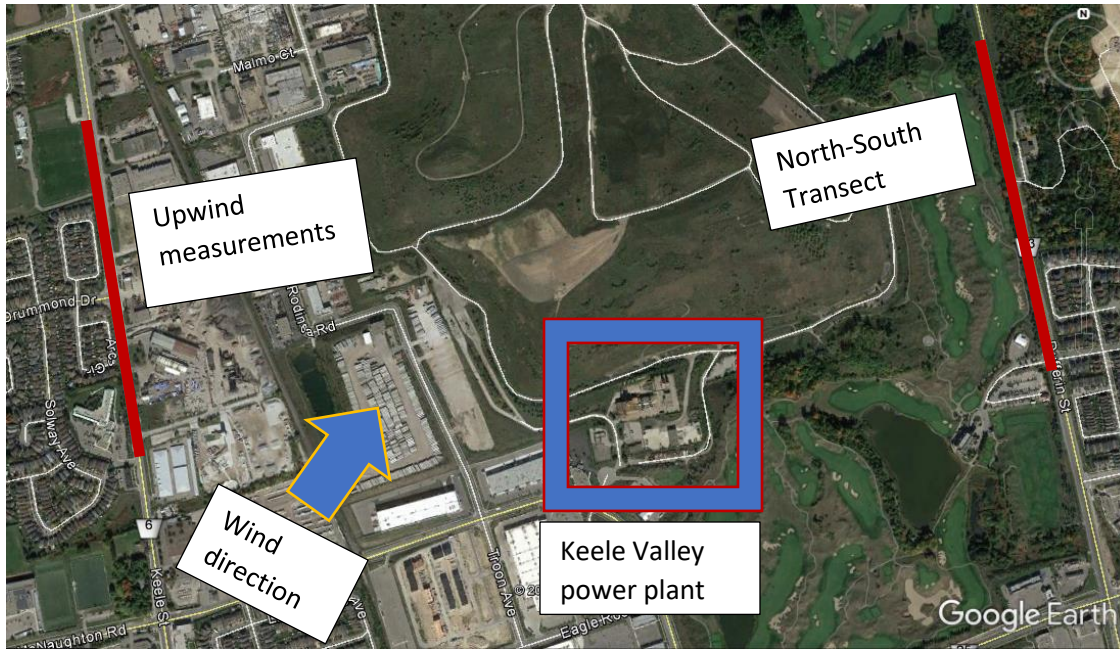


Figure 3.11 Map of the landfill site in the mobile study (March 09,2017)

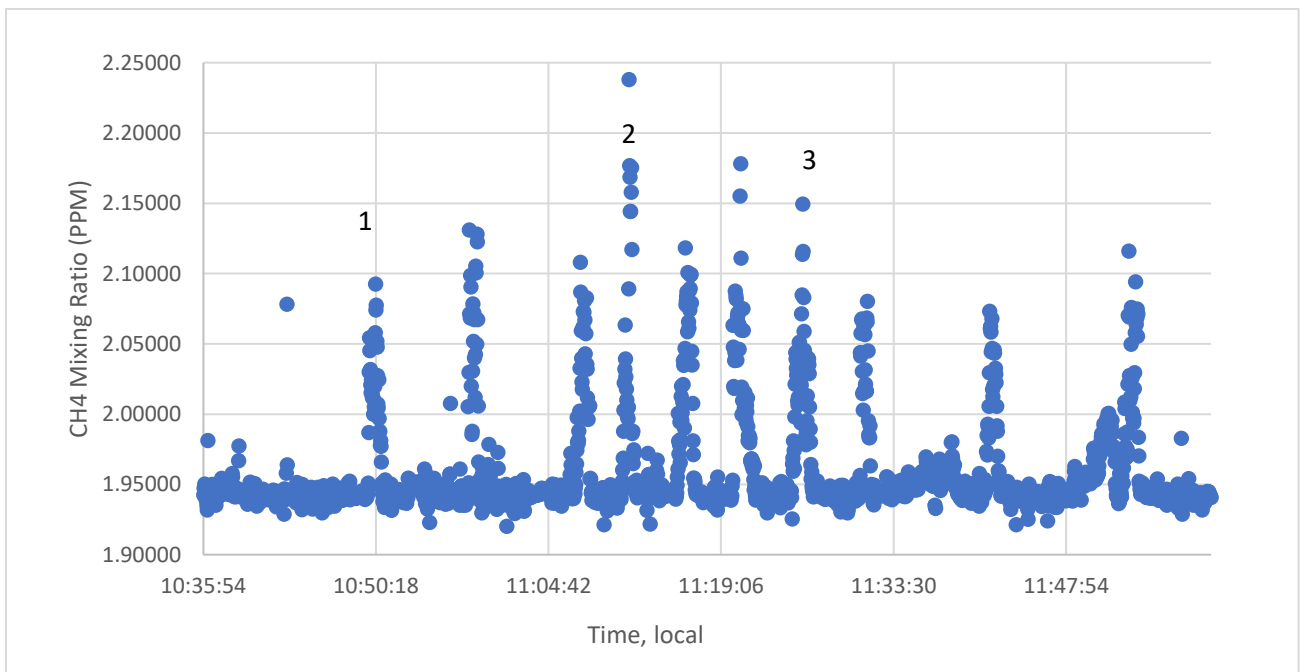


Figure 3.12; Time series plot of methane for landfill study on 09.03.17;

Table 3.6: Flux information for landfill study on 09.03.17;

Transect #	Wind direction, (°) (±10m)	Wind speed, m/s (±0.1)	Transect length, km	Planetary boundary layer, m (±300m)	Cosine theta value	CH4 flux, (×10 <sup>3</sup> Kg/hr)
1 (North-South)	280	2.6	3.193	1000	0.939	6.7
2 (North-South)	280	2.6	2.616	1000	0.939	8.3
3 (North-South)	280	2.6	2.885	1000	0.939	9.8

The combination of a relatively well mixed atmosphere and a stable boundary layer height gave us a more quantitative horizontal flux estimate for methane. Using the mass balance technique explained in section 3.1.1, the horizontal flux estimate on March 09 was  $8.3 (\pm 1.7) \times 10^3$  kg/hr, with a minimum emissions estimate of  $6.7 \times 10^3$  kg/hr and a maximum of  $9.8 \times 10^3$  kg/hr.

The two most significant sources of error in our mass balance technique were the wind direction data and the boundary layer height. For our emissions estimate, we mostly relied on data (wind direction and speed) from the weather station at King City, which was approximately 10 km away. Moreover, the data was provided at 1 hour intervals. Our wind speed and wind direction values were an average of the nearest hour before and after the downfield measurements. For instance, if the methane enhancements were measured between 16:15 and 16:25 pm, we averaged the wind data at 16:00 and 17:00 pm. There was often a significant difference between the two hours, which created a large degree of uncertainty in our emissions estimates. The second most important source of uncertainty in our flux values was the boundary layer height. The PBL used in our calculation was an estimate based on aircraft landing and takeoff data from

either Pearson airport, Hamilton airport or Buffalo airport, depending on the availability of data. We used the reported temperature profile of aircraft as they were landing to estimate a boundary layer height. Another assumption made was that the atmosphere was mixed homogeneous throughout the entire mobile study, which is likely not the case. These contributed significantly to the error calculation of the horizontal flux estimates.

According to an emissions inventory of the Keele Valley Landfill site in 2015, the annual emissions of methane produced is 20669 tonnes per year, which corresponds to  $2.4 \times 10^3$  kg/hr (ECCC., 2015). In comparison, the average emissions estimate of our February and March mobile studies is  $6.0 \times 10^3$  kg/hr. The disparity between the inventory value and our flux estimate depends on several factors. The inventory values were reported 2 years ago, whereas our emissions estimate is more up to date. However, the most important source of potential error is how the two values were determined. An emissions inventory is an engineering estimate of emissions originating from a particular source. However, these inventories have been known to under-estimate the true level of emissions, partly due to non-standardized reporting requirements (Krzyzanowski., 2009). In contrast, a flux estimate is a far more reliable method, using real-time CH<sub>4</sub> mixing ratios. Despite the numerous sources of error related to the mass balance technique, it is a viable method of accurately measuring the level of CH<sub>4</sub> concentration from an emissions source, if the uncertainty due to meteorological parameters can be reduced.

#### 4. Conclusion and future work

The purpose of this thesis was to get an emissions estimate of CH<sub>4</sub> from the Keele Valley Landfill Site using a mobile ground based mass balance approach. Once the CH<sub>4</sub> source was identified, a further 2 mobile studies were conducted in February and March to measure a methane emissions estimate. Using the mass balance technique, an average of 8 transects on two separate days gave us a CH<sub>4</sub> emissions estimate of  $6.0 (\pm 1.6) \times 10^3$  kg/hr, which compared to a reported inventory value of  $2.4 \times 10^3$  kg/hr. Future work would involve reducing the uncertainty in the horizontal flux estimate. This would include having a precise value for the boundary layer height by using an instrument such as a LIDAR, a remote sensing method. Moreover, we can reduce the uncertainty in the wind data by having a mobile weather station mounted on the vehicle to measure local wind speed and direction. An significant improvement of this approach would be to model the mixing rate of CH<sub>4</sub> more accurately from the source to the atmosphere, which would reduce any potential over-estimation caused by assuming a homogeneous boundary layer. Another suggestion would be to combine the mobile study with an aircraft measurement, which would give us an emissions estimate that takes into account both the emissions at the surface and at high altitude. We also used the Cavity Ringdown Spectroscopy along with a Unisearch Tunable Diode Laser Absorption spectroscopy to quantitatively measure the methane concentration at York University. An intercomparison study was conducted where both instruments were collecting methane mixing ratio values for three days. The intercomparison showed that the long path measurements by the TDL had much more instrumental noise than the point source CRDS measurement. Although the two instruments agreed within 0.17 ppm, the two instruments had a low level of correlation, as indicated by the low R-squared value. The lack of correlation is mostly attributed to the high background level of methane and the noise in the

TDL. In the future, the correlation would be improved by using a gold retroreflector, which greatly increases the their return beam strength of the TDL. If the gold retroreflector exhibits better sensitivity and a better signal to noise ratio, it could be used to complement the CRDS in emissions estimates. That would help reduce the lack of accurate and reliable estimates of emissions sources. With accurate estimates and improved monitoring, we will be better equipped to deal with the global warming potential of methane around the world

## **5.0 References;**

"Cavity Ring-Down Spectroscopy (CRDS)." Picarro Inc., 2015. Web. 14 Aug. 2015.

"Facility and GHG information"; Environment and Climate Change Canada.,2015. Web. 10 Apr.2017. < [http://ec.gc.ca/ges-ghg/donnees-data/index.cfm?do=facility\\_info&lang=en&ghg\\_id=G10161&year=2015](http://ec.gc.ca/ges-ghg/donnees-data/index.cfm?do=facility_info&lang=en&ghg_id=G10161&year=2015) >.

Gordon, M., et al. (2015), Determining air pollutant emission rates based on mass balance using airborne measurement data over the Alberta oil sands operations., 3745-3765.

Hausmann, P.; Sussmann, R.; Smale, D. Atmospheric Chemistry and Physics Atmos. Chem. Phys. 2016, 16 (5), 3227–3244.

IPCC, 2014: Climate Change 2014: Synthesis Report. Contribution of Working Groups I, II and III to the Fifth Assessment Report of the Intergovernmental Panel on Climate Change [Core Writing Team, R.K. Pachauri and L.A. Meyer (eds.)]. IPCC, Geneva, Switzerland, 151 pp.

Karion., et al. (2013), Methane emissions estimate from airborne measurements over a western United States natural gas field. Geophysical Research Letters 40.16, 4393-397.

Krzyzanowski, J., The Importance of Policy in Emissions Inventory Accuracy— A Lesson from British Columbia, Canada, *Journal of the Air & Waste Management Association*, 59:4 (2009): 430-439

Phillips, G., et al (2013), Mapping urban pipeline leaks: Methane leaks across Boston." *Environmental Pollution* 173 (2013): 1-4

Peischl, J., et al. (2015), Quantifying atmospheric methane emissions from the Haynesville, Fayetteville, and northeastern Marcellus shale gas production regions, *J. Geophys. Res. Atmos.*, 120, 2119–2139,

Ruddiman, William F. "The Anthropogenic Greenhouse Era Began Thousands of Years Ago." *Climatic Change* 61.3 (2003): 261-93.

Sreenivas, G.; Mahesh, P.; Subin, J.; Kanchana, A. L.; Rao, P. V. N.; Dadhwal, V. K.

Atmospheric Chemistry and Physics Atmos. Chem. Phys. 2016, 16 (6), 3953–3967.

Themelis, Nickolas J., and Priscilla A. Ulloa. "Methane generation in landfills." *Renewable Energy* 32.7 (2007): 1243-257

Verhulst, K. R.; Karion, A.; Kim, J.; Salameh, P. K.; Keeling, R. F.; Newman, S.; Miller, J.; Sloop, C.; Pongetti, T.; Rao, P.; Wong, C.; Hopkins, F. M.; Yadav, V.; Weiss, R. F.; Duren, R.; Miller, C. E. *Atmospheric Chemistry and Physics Discussions* 2016, 1–61.